NANO · MICRO small
www.small-journal.com

Ultra-Stable ITO-Free Organic Solar Cells and Modules Processed from Non-Halogenated Solvents under Indoor Illumination

*David Müller, Ershuai Jiang, Laura Campos Guzmán, Paula Rivas Lázaro, Clemens Baretzky, Shankar Bogati, Birger Zimmermann, and Uli Würfel**

Organic Photovoltaics (OPV) is a very promising technology to harvest artificial illumination and power smart devices of the Internet of Things (IoT). Efficiencies as high as 30.2% have been reported for OPVs under warm white light-emitting diode (LED) light. This is due to the narrow spectrum of indoor light, which leads to an optimal bandgap of ≈1.9 eV. Under full sunlight, OPV devices often suffer from poor stability compared to the established inorganic PV technologies such as crystalline silicon. This study focuses on a potentially very cost-effective Indium Tin Oxide (ITO) free cell stack with absorber materials processed from non-halogenated solvents. These organic solar cells and modules with efficiencies up to 21% can already achieve remarkable stabilities under typical indoor illumination. Aging under 50,000 lux LED lighting leads to very little degradation after more than 11 000 h. This light dose corresponds to more than 110 years under 500 lux. For modules encapsulated with a flexible barrier, extrapolated lifetimes of more than 41 years are achieved. This shows that OPV is mature for the specific application under indoor illumination. Due to the large number of potential organic semiconducting materials, further efficiency increase can be expected.

1. Introduction

Emerging photovoltaics (PV) such as organic PV (OPV) and perovskite PV (PPV) have reached remarkable power conversion efficiencies (PCE) in the last years. 15.2% and 24.4% have been certified records and 19.2% and 26.0% confirmed efficiencies for OPV and PPV, respectively.[1,2] Not only for outdoor use cases these thin film technologies are very interesting but also for indoor light harvesting. The bandgap of these semiconductors can be tailored for efficient conversion of artificial indoor light into electricity. With minor differences between various lamp types (LED, fluorescent lamp, etc.) and respective emission spectra the optimal bandgap was calculated to be in the range of 1.8–2.0 eV.[3,4] Comparing efficiencies under indoor light conditions is still challenging but several proposals for best practice have been adopted recently.[3,5,6] For OPV with PB2:FTCC-Br under 1000 lux 30.2%, with PM6:Y6-O 29.4% under 700 lux and 26.1% with PM6:IO-4Cl under 1000 lux warm white LED light was presented.[7–9] For ITO-free organic solar cells and absorbers processed from non-halogenated solvents 19.3% have been shown under 500 lux cold white LED light using PV-X plus as absorber material.[3] Similarly, as for outdoor solar cells and modules the stability indoors is a crucial point for acceptance and reliability in real products, i.e., towards commercialization. As one of the largest benefits is to overcome the use of batteries and especially their replacement, the PV device has to exhibit lifetimes in the same range as the product which it is supplying with electrical energy. Indoor PV profits from rather mild environments with typically no UV-light contribution, lower irradiances, lower and much more constant temperatures and moisture levels. Depending on the application (industry) more extreme settings might be reasonable. Although the conditions will be less harsh in general it has to be proven that the solar cells and modules can be durable in such environments. Only a few studies show detailed data on the stability under indoor conditions and usually only for short time periods. If under simulated sunlight solar cells do not degrade, e.g., for several thousands of hours, it might be assumed that under the milder (indoor) conditions the devices

D. Müller, L. Campos Guzmán, P. Rivas Lázaro, S. Bogati, B. Zimmermann, U. Würfel
Fraunhofer Institute for Solar Energy Systems ISE
Heidenhofstr. 2, 79110 Freiburg, Germany
E-mail: uli.wuerfel@ise.fraunhofer.de

D. Müller, C. Baretzky, U. Würfel
Freiburg Materials Research Center FMF
University of Freiburg
Stefan-Meier-Str. 21, 79104 Freiburg, Germany

E. Jiang, U. Würfel
Cluster of Excellence livMatS
University of Freiburg
Georges-Köhler-Allee 105, 79110 Freiburg, Germany

The ORCID identification number(s) for the author(s) of this article can be found under https://doi.org/10.1002/smll.202305437

DOI: 10.1002/smll.202305437

would also not degrade. However, this is not always valid and has to be investigated individually. Ramírez–Como et al. studied the degradation of rigid ITO-based 0.09 cm^2 organic solar cells with p-DTS(FBTTh2)$_2$:$PC_{70}BM$ processed from chlorobenzene as an absorber layer under warm white LED and simulated AM1.5G light, respectively. Timespans after which the initial efficiency has dropped to 80% (T_{80}) of about 1000 h at 1000 lux LED light are shown, while under "1 sun" (simulated AM1.5G, corrected for spectral mismatch) illumination T_{80} times between 2000 h and 3500 h can be extracted.[10] Lee et al. showed thermal stability data upon aging at 45° C in the dark. Under 1000 lux cold white LED light 11.3% and 15% for PBDB-T:PCBM and PBDB-T:ITIC-Th based solar cells were measured, respectively. After 720 h 95% and 85% of the initial PCE was maintained for the non-fullerene and the fullerene device, respectively. Also after about 350 h of weak LED illumination the PCE remained unchanged for both absorber types.[11] Bai et al. fabricated rigid 0.07 cm^2 ITO-based solar cells with D18:FCC-Cl as absorber coated from chloroform and achieved 28.8% under 500 lux warm white LED light. The encapsulated devices were aged for 500 h at 500 lux white LED light and maintained 95% of their initial performance. The authors attributed the loss to an imperfect encapsulation.[12] Cui et al. presented with PM6:IO-4Cl processed from chlorobenzene on ITO glass substrates efficiencies up to 24.6% under 500 lux warm white LED light for 1 cm^2 solar cells. In the first 1000 h under "indoor light" no degradation was observed.[8] Park et al. investigated the thermal stability of PBDB-TSCl:IT-4F and PBDB-T:IT-4F based solar cells under 100°C for 34 h and showed 5% and 25% drop in efficiency, respectively.[13] Cui et al. reported decent efficiencies for 1 cm^2 rigid ITO-based PM6:fullerene and non-fullerene solar cells processed from chlorobenzene between 17.2% and 21.2% under 500 lux warm white LED light. The stability of encapsulated devices was investigated under warm white LED light with 500 lux intensity and after 500 h more than 90% of the initial efficiency are maintained.[14] Thermal degradation at 45° C in the dark led to a 20% drop in the first 160 h.

Further notable studies on stability under different aging conditions but not explicitly measured under indoor conditions will be briefly described below.

Greenbank et al. conducted accelerated aging experiments with cycled illumination at 0.1 and "1 sun" on rigid 0.5 cm^2 ITO-based PCE12:ITIC solar cells. After the first 6 h at "1 sun" 40% of the efficiency is lost, and the 0.1 sun illumination sample follows the same trend at a slower speed.[15] A T_{80} time corresponding to less than 0.5 years under 500 lux could be estimated, however, as no UV filter was used the degradation might be more pronounced compared to pure white LED aging. Lee et al. published T_{80} times of ≈500 h under continuous AM1.5G illumination for ITO-based rigid solar cells with PTB7-Th:IEICO-4F:$PC_{71}BM$ as an absorber material. Furthermore, for the same solar cells after 500 h of 85° C treatment, almost no loss was recorded.[16] Yang et al. showed thermally stable PM6:BTTT-2Cl solar cells with a polymer acceptor additive PZ1.[17] After 800 h at 110° C (150° C) 95% (88%) of the initial PCE was maintained. Sun et al. reported photo and thermal stability on ITO-based organic solar cells with J71:ITC6-IC as absorber material, coated from chloroform in air in bulk hetero-junction (BHJ) and layer-by-layer (LbL) architecture. Under continuous "1 sun" illumination (intensity not specified) the BHJ (LbL) device showed a PCE reduction of 32% (15%) within 500 h. At 120° C under inert conditions, the LbL (BHJ) device performance was reduced by 12% (19%) after 1500 h.[18] Subramaniam et al. investigated the stability of OPV devices under thermal and light stress. T_{80} times of ≈40 h under 120° C for encapsulated organic solar modules were achieved. In damp/heat (65° C/85% rH) T_{80} times of ≈4000 h were shown for low water vapor transmission rate (WVTR) barriers. Under continuous simulated AM1.5G illumination, T_{80} times of ≈500 h and 2250 h were presented for samples kept at open-circuit and maximum-power point conditions, respectively.[19]

Further work reported in literature includes investigation of the photo-stability,[20–31] stability with respect to interfaces,[27,30,32–34] encapsulation,[35–39] morphological stability (single material, side-chain engineering, structural hindrance...),[24,25,28,40,41] thermal stability,[23,25,29,31,40,42,43] mechanical stability,[44,45] and accelerated lifetime testing,[30,40,46,47] carried out with the main focus on outdoor application. Moreover, there are a number of comprehensive reviews summarizing the work on long-term stability of organic photovoltaic devices.[33,48–53]

This work focuses on the investigation and optimization of photo- and thermally stable OPV for indoor applications. Screening different promising absorber materials which have shown decent efficiencies on an ITO-free solar cell stack are used and interlayer and encapsulation materials and methods are varied. Acceleration in both light and temperature is used to estimate the lifetime of rigid and flexible solar cells and modules under indoor conditions.

2. Results

2.1. Accelerated Aging under LED Illumination

To investigate the light-induced degradation of ITO-free organic solar cells for indoor use cases a custom set of individual aging chambers was developed. Each chamber is equipped with cold white LEDs (ZFS-85000HD-CW from JKL Components). The corresponding spectrum is shown in Figure S1 (Supporting Information). The temperature inside the aging chambers is maintained at room temperature (by cooling via a heat sink and fans) and tracked by a digital thermometer (SBS-DL-123 from Steinberg Systems), see Figure S2a (Supporting Information). The humidity is tracked but not explicitly controlled, however it follows the laboratory values and represents a quite typical indoor condition (between 20% and 50% relative humidity, depending on the chamber temperature), see Figure S2b (Supporting Information). The aging chambers are protected against ambient light using light tight housing. The inner walls are covered with reflective material to increase the homogeneity of the illumination, see Figure S3 (Supporting Information) for the intensity distribution. Relative differences in intensity below 10% are achieved, c.f. Table S1 (Supporting Information). In total four different levels of illuminance were set, 500, 2,000, 10,000 and 50,000 lux which represents a maximum light acceleration factor of 100 with respect to 500 lux. **Figure 1** shows the aging chambers and their configurations.

The solar cells were aged under open-circuit conditions and current density voltage (*JV*) measurements were performed regularly under 500 lux in our indoor LED setup as presented

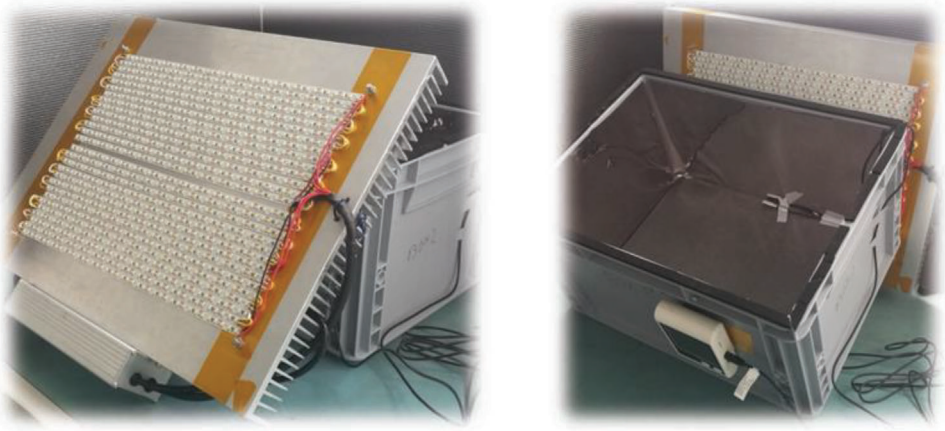

Figure 1. LED based aging setup with temperature and humidity tracking.

previously.[3] The LED spectrum, the integrated current-density at 500 lux as well as the external quantum efficiency (EQE) are shown in Figure S1 (Supporting Information). Open circuit condition during aging was selected as it was found to show typically the strongest/fastest degradation.[19,54–57] It resembles then the worst-case scenario and devices operated under more realistic, e.g., maximum power point condition might perform better, and maintain efficiency for longer time. Degradation mechanisms promoted by accumulated charge carriers would be stronger at open-circuit condition.[56]

As a first absorber material TPD-3F:IT-4F was used.[3,58] For all full chemical names and further processing information we refer to the methods section and Table S2 (Supporting Information). The solar cell stack is based on our low-cost ITO-free electrode: (glass)substrate/AZO/Al/AZO/ZnO/absorber/HTL-5.[3,59,60] As a protection against oxygen, water vapor, and mechanical impacts the solar cells were encapsulated with a UV-curable epoxy (≈300 µm thick, Katiobond LP655 from Delo) and a glass lid. **Figure 2** shows the photovoltaic figures of merit obtained at 500 lux cold white LED light as a function of the aging time on a

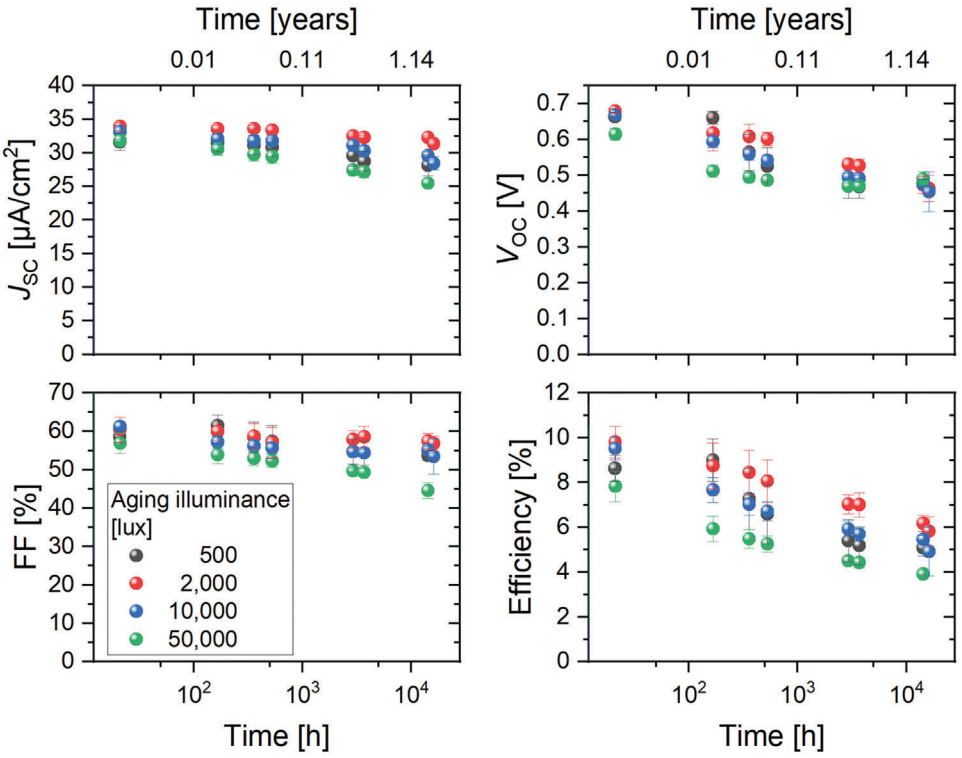

Figure 2. Photovoltaic figures of merit for 0.1 cm² ITO-free rigid solar cells with TPD-3F:IT-4F as an absorber layer as a function of ageing time for four different levels of illuminance. The *JV* measurements were carried out at 500 lux.

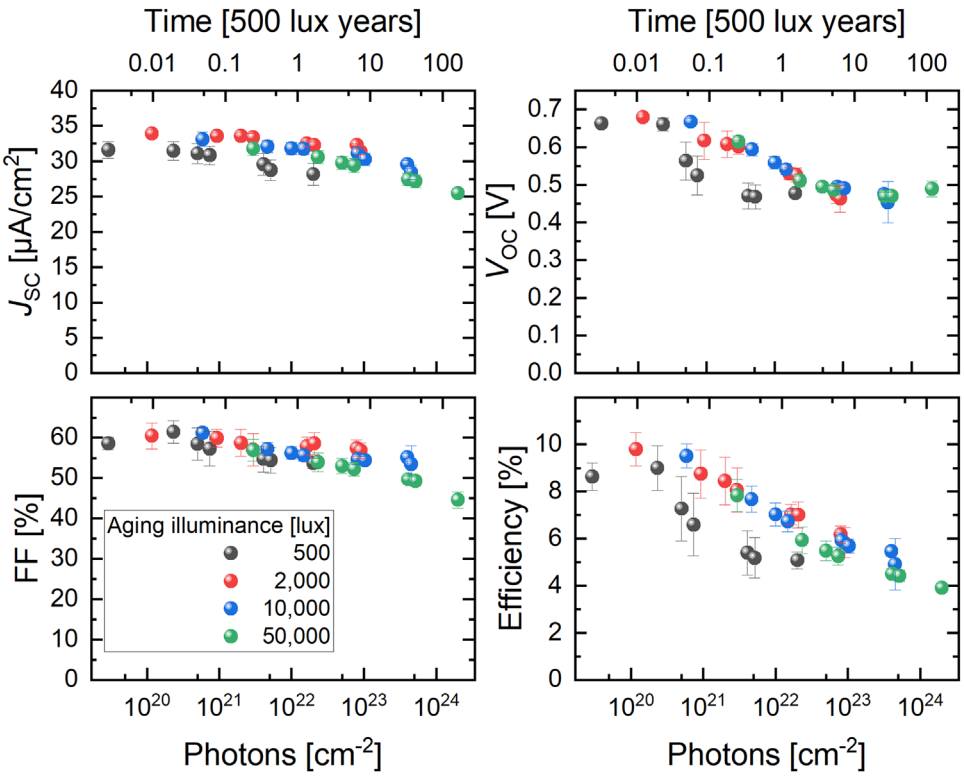

Figure 3. Photovoltaic figures of merit for 0.1 cm² ITO-free rigid solar cells with TPD-3F:IT-4F as an absorber layer as a function of the number of incident photons for four different levels of illuminance during the aging process. The *JV* measurements were carried out at 500 lux.

logarithmic time axis for the different levels of illuminance (six individual solar cells per illuminance).

It is observed that with increasing illuminance the solar cells degrade faster, with the sample aged at 500 lux being an exception. As for all other intensities, the samples show a very comparable behavior, we attribute this stronger (faster) degradation of the 500 lux sample to an imperfect (manual) encapsulation process. For better comparison and visualization, the illumination time t was converted into a photon dose $\theta(t)$ each solar cell has received at a certain time;

$$\theta\ (t) = t \int_0^\infty \varphi\,(\lambda)\ d\lambda \tag{1}$$

where, $\varphi(\lambda)$ denotes the photon current density of the LED at a certain illuminance as a function of wavelength λ. The data from Figure 2 is replotted with the new axis in **Figure 3**.

Now the data points in the efficiency plot from different illuminances lay all on a straight line (again, except for the sample aged under 500 lux) indicating an accelerated aging process. Additionally, the top abscissa relates the number of photons to a time corresponding to years under 500 lux. In general, this particular solar cell stack is not very stable, and losses are composed of losses in short-circuit current density (J_{SC}), fill factor (*FF*) and open-circuit voltage (V_{OC}). While J_{SC} and *FF* degrade moderately, V_{OC} losses are more dominant up to 10^{23} photons cm^{-2} after which the value of V_{OC} levels.

With PV-X plus[3,61] as photoactive material in a slightly different cell stack ((glass)substrate/AZO/Al/AZO/absorber/HTL-X/HTL-5) aged under similar conditions has led to the performance evolution depicted in **Figure 4**. For comparison, the initial performance of the different solar cells (absorber materials, substrate types and areas) is summarized in **Table 1**. This time, 12 individual solar cells were examined for each illuminance. With the PV-X plus absorber material in this solar cell stack, extremely stable devices can be fabricated. Even after more than one year of light exposure under 50 klux — corresponding to more than 100 years of the photon dose under 500 lux — almost no loss is observed. Importantly, no noticeable differences are observed between the different aging illuminances, although the accumulated photon dose (Figure 4) differs up to a factor of 100. Thus, it can be concluded that there is no photo-induced degradation effect occurring within the investigated period of time. This can be seen even more clearly in Figures S4 and S5 (Supporting Information). This is a very promising result. Whether such long lifetimes of, e.g., 100 years and more under 500 lux can be achieved in real-time (i.e., without acceleration) is obviously mainly a question of encapsulation. So far, we can state at least that the intrinsic photostability enables such long lifetimes.

As PM6:IO-4Cl[3,8] is a very suitable material for converting cold white LED light into electrical energy it was investigated in a similar way under 50,000 lux. The results are depicted in **Figure 5** comparing them to PV-X plus and TPD-3F:IT-4F. The PM6:IO-4Cl based solar cells lose efficiency comparably fast, similar as TPD-3F:IT-4F. However, the degradation is dominated by losses in J_{SC} and *FF* while V_{OC} remains relatively stable, see Figure S6 (Supporting Information) for details on the development of the individual parameters for PM6:IO-4Cl devices. Furthermore, the

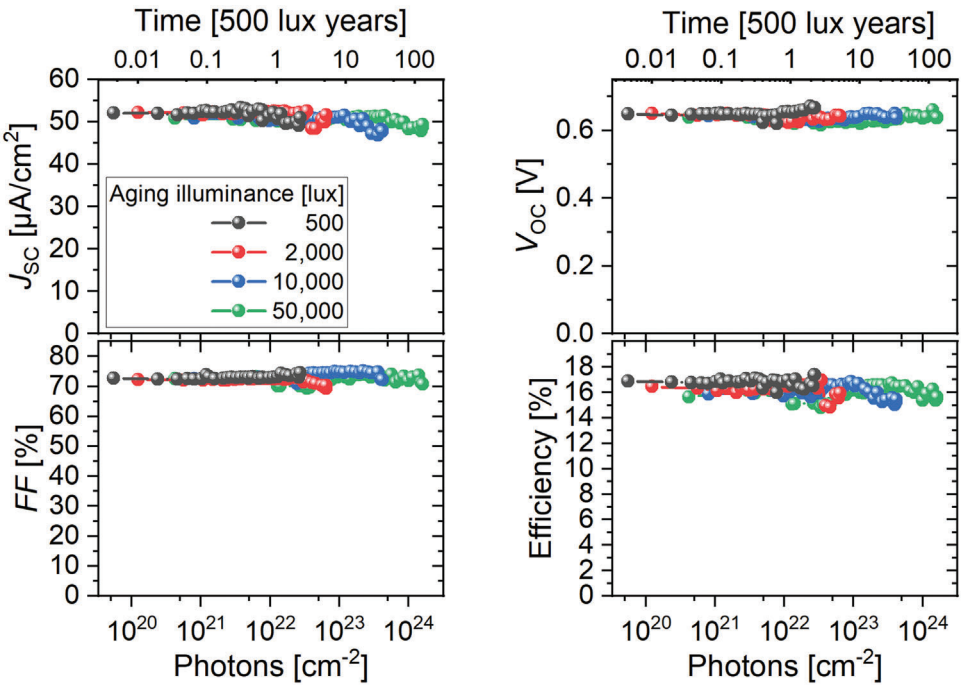

Figure 4. Photovoltaic figures of merit as a function of incident photons for 0.1 cm^2 ITO-free rigid solar cells with PV-X plus absorber aged under four different levels of illuminance. The JV measurements were carried out at 500 lux.

T_{80} values, (time after which the efficiency has dropped to 80% of the initial value after encapsulation) corresponding to the photon dose under 500 lux are indicated in the graph. As mentioned previously for PV-X plus virtually no decrease in the photovoltaic performance parameters is observed, for a photon dose that corresponds to more than 100 years under 500 lux. For TPD-3F:IT-4F and PM6:IO-4Cl, a relative 20% drop in efficiency is reached after a photon dose that corresponds to 1.5 and 4.1 years under 500 lux illumination, respectively.

Rigid small area solar cells with rigid encapsulation are the first step in the chain of investigation towards stable OPV devices for indoor light harvesting. Although several applications will not need flexible devices, it is one of the beneficial properties of thin film photovoltaics to be potentially flexible and high throughput low-cost roll-to-roll processing requires at least a flexible carrier for the device production. Thus, we also investigated the degradation of 1.1 cm^2 flexible solar cells under 50,000 lux cold white LED light. PV-X plus was used as an absorber since it was the most stable of the three active materials investigated herein. The rigid glass substrate was replaced by a flexible barrier film UBF512 (203 µm thick, from 3 M) and the encapsulation stack was

Table 1. Initial (after encapsulation, prior to light exposure) photovoltaic parameters of the respective solar cells and modules, measured under 500 lux cold white LED light. For the 8.1 cm^2 modules the average per cell stripe (area) values are given in parentheses for V_{OC} and J_{SC}. PCE max denotes the maximum efficiency which was achieved with this solar cell stack.

Material	J_{SC}	V_{OC}	FF	PCE	PCE max.	Area
	[µA cm^{-2}]	[V]	[%]	[%]	[%]	[cm^2]
PV-X plus	50.9	0.636	74.4	16.9	19.9	0.1
PV-X plus flexible	48.9	0.685	75.0	17.7	18.5	1.1
PV-X plus module	7.03 (56.2)	5.137 (0.641)	71.6	18.2	18.2	8.1
PM6:IO-4Cl	36.2	0.993	69.1	17.3	21.3	0.1
TPD-3F:IT-4F	34.7	0.686	64.2	10.6	19.5	0.1

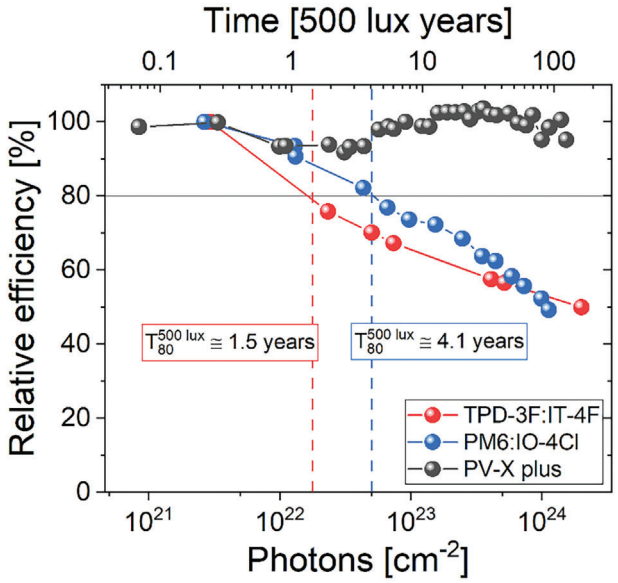

Figure 5. Relative efficiency at 500 lux for 0.1 cm^2 ITO-free rigid solar cells with either PV-X plus, TPD-3F:IT4F or PM6:IO-4Cl as an absorber layer, respectively as a function of the incident photons for ageing at 50,000 lux. Dashed lines and corresponding numbers denote the T_{80} times corresponding to the photon dose under 500 lux.

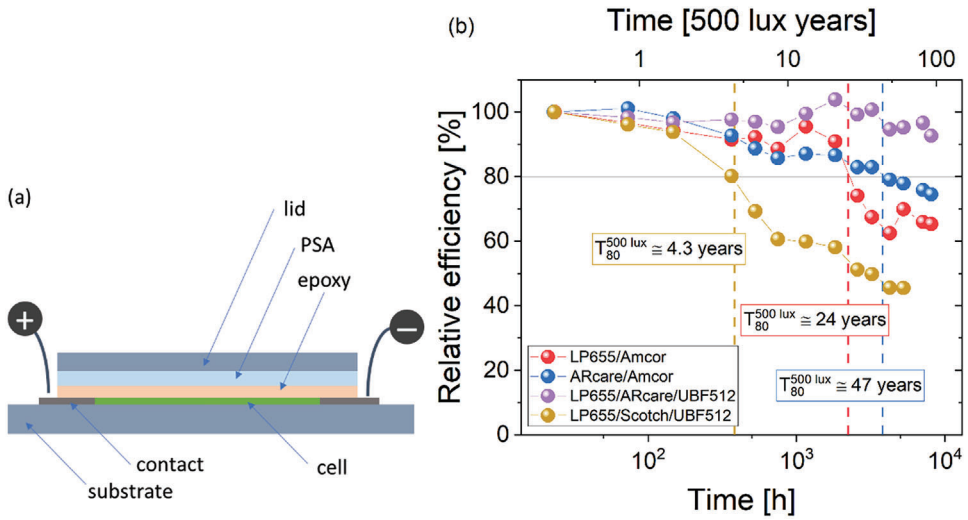

Figure 6. a) Schematic of the encapsulation stack. b) Relative efficiency at 500 lux for 1.1 cm2 ITO-free flexible (UBF512) solar cells with PV-X plus as the absorber layer and different encapsulation stacks, as a function of the incident photons. Dashed lines and corresponding numbers denote the T80 times in years at 500 lux.

varied. As barriers UBF512 and SOLARS-AUGW (100 µm thick, from Amcor Flexibles) and as sealants Katiobond LP655 and ARcare 92734 (25 µm thick, pressure sensitive adhesive, (PSA), from Adhesive Research) as well as Scotch PSA (from 3 M) were used, see **Figure 6**a,b shows the relative efficiency for the aged devices. The best stability was obtained with an encapsulation stack of Katiobond LP655/ARcare 92734/UBF512. After more than 8,000 h under 50,000 lux LED light (corresponding to the same number of photons under 500 lux after ≈92 years) more than 90% of the initial efficiency is maintained. Faster degradation is observed for the case with the Scotch PSA but else similar encapsulation stack. Here a T_{80} time of only 4.3 years was extracted. In contrast to the Scotch PSA the ARcare 92734 has a moderate moisture barrier (2.2 g m^{-2}/day) and it highlights the importance of the barrier properties of the adhesion layer. Using SOLARS-AUGW although having higher water vapor transmission rate (WVTR) of 0.003 g m^{-2}/day compared to UBF512 (WVTR 6×10^{-5} g m^{-2}/day) and moreover being thinner by a factor of four, thus much more flexible, still decent indoor stabilities could be achieved. For encapsulation stacks with Katiobond LP655/ARcare 92734/ SOLARS-AUGW and ARcare 92734/SOLARS-AUGW, T_{80} times of 2,500 h and 4,300 h (corresponding to the number of photons under 500 lux after 24 years and 74 years), respectively were achieved. The full set of PV figures of merit can be found in Figure S7 (Supporting Information).

The excellent results with respect to performance and stability of organic solar cells under indoor light could be transferred to the module level. **Figure 7** shows the relative PCE of 8.1 cm^2 modules with eight interconnected cells in series and PV-X plus absorber aged under 10,000 and 50,000 lux, respectively, see also Figure S8 (Supporting Information) for the other photovoltaic parameters. Aiming towards flexible devices the modules were encapsulated with two different stacks, Katiobond LP655/UBF512 or ARcare 92734/SOARS-AUGW, the first with the perspective of higher barrier properties and the latter with focus on higher

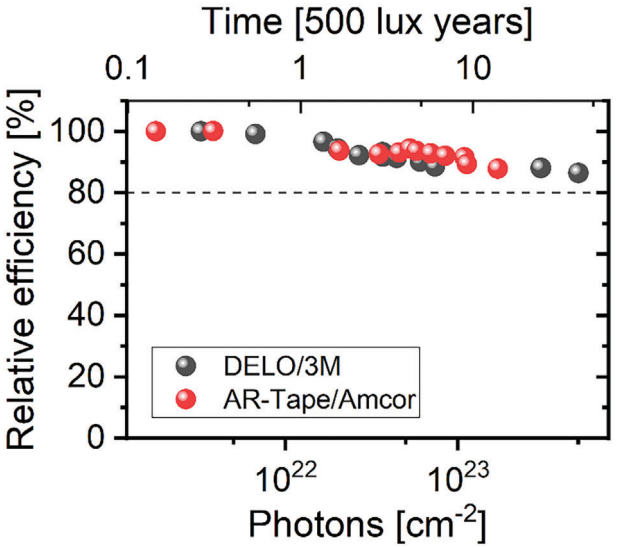

Figure 7. Relative efficiency at 500 lux for rigid 8.1 cm2 modules with PV-X plus as the absorber layer and an AR-Tape/Amcor (DELO Katiobond LP655/UBF512) encapsulation, aged under 10,000 (50,000) lux as a function of the number of incident photons. The corresponding 500 lux time is given in the top abscissa. The horizontal line indicates the 80% level with respect to the first measurement which was not reached until now (≈6,100 h and 3,600 h, respectively).

flexibility. After 3,600 h at 50,000 lux and 6,100 h at 10,000 lux the devices with SOLARS-AUGW and UBF512, respectively still have more than 80% of the initial efficiency. The corresponding 500 lux equivalent years are 41 and 13.9, respectively.

2.2. Thermal Aging

A second important degradation factor of organic solar cells is heat.[17,19,34,62–66] Although typical indoor conditions are expected

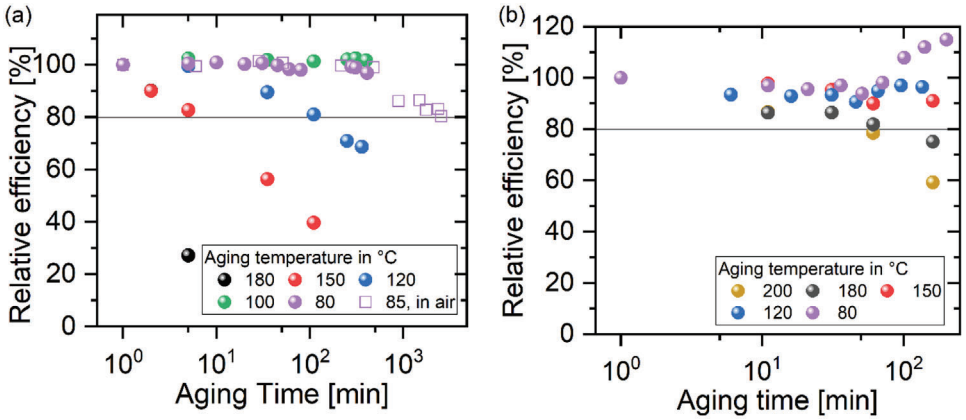

Figure 8. Relative efficiency at 500 lux cold white LED light for 0.1 cm^2 ITO-free rigid solar cells with a) PV-X plus and b) PM6:IO-4Cl absorber layer as a function of the aging time at different temperatures.

to be around room temperature, elevated temperature environments in industrial use cases are reasonable. To investigate thermally induced degradation, aging experiments under different temperatures were carried out on two different non-fullerene absorber systems.

Unencapsulated PV-X plus and PM6:IO-4Cl-based ITO-free solar cells were exposed to temperatures between 80 and 200° C under inert conditions in the dark. **Figure 8** shows the relative efficiency as a function of the aging time obtained under 500 lux cold white LED light at room temperature (see Figures S9 and S10, Supporting Information for the full PV figures of merit). Encapsulated cells thermally aged in an oven in air show a comparable trend, see the purple squares in Figure 8a. For PV-X plus (PM6:IO-4Cl) temperatures up to 100 (150)° C cause no significant degradation in the first 400 (200) min. For longer exposures to 85° C the PV-X plus device also decreases below 80% of the initial efficiency and a T_{80} time of 2,560 h is obtained.

Using the T_{80} times from the PV-X plus based solar cells an Arrhenius plot could be created, see Figure S11 (Supporting Information). The extracted T_{80} times lay on a straight line in this representation thus it can be concluded that by increasing the temperature the degradation upon temperature can be accelerated in this manner. Furthermore, lifetimes at lower temperatures of more than 10 (50) years at 50 (40)° C could be extrapolated. The activation energy was calculated to be 1.1 eV. The degradation upon thermal stress could be attributed to the changes in the morphology of the active layer, such as demixing of the domains, leading to larger pure acceptor or donor phases. In turn, the exciton dissociation can be hindered which is reflected in a lower J_{SC} and V_{OC} and ultimately in a reduced efficiency. Ghasemi et al. analyzed several modern non-fullerene-based organic solar cells and investigated the diffusion coefficient. For PM6:Y6 or PTB7-Th:IEICO-4F activation energies of ≈1.4 eV or 2 eV, respectively were presented for the diffusion coefficient.[67] A detailed analysis of the activation energy and the underlying mechanism is beyond the scope of this work.

3. Conclusion

In summary, we present remarkably stable ITO-free organic solar cells and modules with absorber layers coated from non-halogenated solvents aged under different illumination intensities and thermal stress. Even after photon dose corresponding to more than 100 years (90 years) under 500 lux, nearly no degradation was observed when using PV-X plus as photoactive material on rigid (flexible) substrates. For comparison, the same photon dose corresponds to ≈1,900 h under "1 sun". It must be noted though, that real-time effects such as temperature variations or occasional outdoor light (e.g., UV light) have to be considered in real applications. The latter can however be avoided by appropriate filters. Against thermal stress devices with PV-X plus also show considerable robustness, maintaining 80% of their initial efficiency for more than 2500 h at 85° C. Our results demonstrate that organic photovoltaics provide high efficiency and remarkable long-term stability under artificial light and are thus best suited and mature for indoor applications.

4. Experimental Section

Device Fabrication: The ITO-free cell fabrication process started with glass substrates. After the cleaning in ultrasonic baths of acetone, isopropanol, and deionized water for 10 min each and subsequent nitrogen dry blowing an Al-based metal electrode system was deposited via sputtering with a shadow mask. As ETL (TPD-3F:IT-4F and PM6:IO-4Cl devices only) a 15 nm ZnO (1% N11 from Avantama, diluted in isopropanol) was spin-cast in air, transferred into a nitrogen filled glove box (GB) and annealed for 5 min at 120° C. A 130 (120, 150) nm film of PV-X plus from RaynergyTek (TPD-3F:IT-4F from RaynergyTek, PM6:IO-4Cl from 1-Material) spin-cast from o-xylene (o-xylene, chlorobenzene) at room temperature followed by 5 (5, 10) min annealing at 120 (120, 160)° C formed the active layer, respectively. The HTL was formed by a double layer of PEDOT:PSS (30 nm PV-HTL-X and 50 nm PV-HTL-5, from RaynergyTek, the sheet resistance is 795±137 Ω) spin-cast in a nitrogen filled GB and dried for 5 min at 110° C in the GB. To electrically contact, a support structure consisting of 5 nm Cr and 100 nm Ag was deposited via e-beam and thermal evaporation, respectively, at a pressure below 10^{-5} mbar with a shadow mask. Rigid solar cells were encapsulated using UV curable epoxy and glass covers as barrier. Flexible devices were laminated to the barrier films using pressure sensitive adhesives and/or epoxy, all steps performed in the GB. All flexible films were degassed prior to use for 30 min at 100° C in the GB.

Device Characterization: Current voltage measurements at 1000 W m-2 simulated AM1.5G light with a class A solar simulator (Newport SP94063A-SR1-167) and at several illuminances with a cold white LED

array (Brandmeier LTAS-100/1). In the case where the active area is not well defined, black shadow masks are used to limit the aperture area precisely. The error compared to measure without a mask is about up to 10%. Data is recorded with a programmed Keithley 2400 source measuring unit. For LED measurements the whole setup is protected against ambient light. The indoor irradiance and illuminance are determined according to Cui et al.[5] and by using a calibrated reference diode (S2282 Hamamatsu) and a certified reference solar cell (RS-ID-4), respectively. The traceability of the measurement of the spectral distribution of the LEDs to SI-Units is achieved using a standard lamp for the calibration of the spectroradiometer. The traceability of the measurement of the irradiance to SI-Units is realized with a primary reference solar cell. Both, standard lamp as well as reference solar cell are calibrated by the Physikalisch-Technische Bundesanstalt (PTB), the National Metrology Institute of Germany.

Supporting Information

Supporting Information is available from the Wiley Online Library or from the author.

Acknowledgements

The authors acknowledge the funding from the German Federal Ministry for Economic Affairs and Energy (FKz. 03EE1007 – Organaut). E.J. and U.W. acknowledge the Cluster of Excellence livMatS: Funded by the Deutsche Forschungsgemeinschaft (DFG, German Research Foundation) under Germany's Excellence Strategy—EXC-2193/1—390951807.

Open access funding enabled and organized by Projekt DEAL.

Conflict of Interest

The authors declare no conflict of interest.

Data Availability Statement

The data that support the findings of this study are available from the corresponding author upon reasonable request.

Keywords

IoT, indoor, organic solar cells, photovoltaics, stability

Received: July 7, 2023
Revised: October 7, 2023
Published online:

[1] U. Würfel, J. Herterich, M. List, J. Faisst, M. F. M. Bhuyian, H.-F. Schleiermacher, K. T. Knupfer, B. Zimmermann, *Sol. RRL* **2021**, *5*, 651.
[2] M. A. Green, E. D. Dunlop, M. Yoshita, N. Kopidakis, K. Bothe, G. Siefer, X. Hao, *Prog. Photovoltaics* **2023**, *31*, 651.
[3] D. Müller, L. Campos Guzmán, E. Jiang, B. Zimmermann, U. Würfel, *Sol. RRL* **2022**, *6*, 2200175.
[4] M. Freunek, M. Freunek, L. M. Reindl, *IEEE J. Photovoltaics* **2013**, *3*, 59.
[5] Y. Cui, L. Hong, T. Zhang, H. Meng, H. Yan, F. Gao, J. Hou, *Joule* **2021**, *5*, 1016.
[6] D. Lübke, P. Hartnagel, J. Angona, T. Kirchartz, *Adv. Energy Mater.* **2021**, *11*, 2101474.
[7] L.-K. Ma, Y. Chen, P. C. Chow, G. Zhang, J. Huang, C. Ma, J. Zhang, H. Yin, A. M. Hong Cheung, K. S. Wong, S. K. So, H. Yan, *Joule* **2020**, *4*, 1486.
[8] Y. Cui, Y. Wang, J. Bergqvist, H. Yao, Y. Xu, B. Gao, C. Yang, S. Zhang, O. Inganäs, F. Gao, J. Hou, *Nat. Energy* **2019**, *4*, 768.
[9] T. Zhang, C. An, Y. Xu, P. Bi, Z. Chen, J. Wang, N. Yang, Y. Yang, B. Xu, H. Yao, X. Hao, S. Zhang, J. Hou, *Adv. Mater.* **2022**, *34*, 2207009.
[10] M. Ramírez-Como, A. Sacramento, J. G. Sánchez, M. Estrada, J. Pallarès, V. S. Balderrama, L. F. Marsal, *Sol. Energy Mater. Sol. Cells* **2021**, *230*, 111265.
[11] C. Lee, A. Yi, H. J. Kim, M. Nam, D.-H. Ko, *Adv. Energy Sustainability Res.* **2021**, *2*, 2100041.
[12] F. Bai, J. Zhang, A. Zeng, H. Zhao, K. Duan, H. Yu, K. Cheng, G. Chai, Y. Chen, J. Liang, W. Ma, H. Yan, *Joule* **2021**, *5*, 1231.
[13] S. Park, H. Ahn, J.-Y. Kim, J. B. Park, J. Kim, S. H. Im, H. J. Son, *ACS Energy Lett.* **2020**, *5*, 170.
[14] Y. Cui, H. Yao, T. Zhang, L. Hong, B. Gao, K. Xian, J. Qin, J. Hou, *Adv. Mater.* **2019**, *31*, 1904512.
[15] W. Greenbank, N. Djeddaoui, E. Destouesse, J. Lamminaho, M. Prete, L. Boukezzi, T. Ebel, L. Bessissa, H.-G. Rubahn, V. Turkovic, M. Madsen, *Energy Technol.* **2020**, *8*, 2000295.
[16] J. Lee, J.-H. Lee, H. Yao, H. Cha, S. Hong, S. Lee, J. Kim, J. R. Durrant, J. Hou, K. Lee, *J. Mater. Chem. A* **2020**, *8*, 6682.
[17] W. Yang, Z. Luo, R. Sun, J. Guo, T. Wang, Y. Wu, W. Wang, J. Guo, Q. Wu, M. Shi, H. Li, C. Yang, J. Min, *Nat. Commun.* **2020**, *11*, 1218.
[18] R. Sun, J. Guo, Q. Wu, Z. Zhang, W. Yang, J. Guo, M. Shi, Y. Zhang, S. Kahmann, L. Ye, X. Jiao, M. A. Loi, Q. Shen, H. Ade, W. Tang, C. J. Brabec, J. Min, *Energy Environ. Sci.* **2019**, *12*, 3118.
[19] S. V. Subramaniam, D. Kutsarov, T. Sauermann, S. B. Meier, *Energy Technol.* **2020**, *8*, 2000234.
[20] A. J. Clarke, J. Luke, R. Meitzner, J. Wu, Y. Wang, H. K. H. Lee, E. M. Speller, H. Bristow, H. Cha, M. J. Newman, K. Hooper, A. Evans, F. Gao, H. Hoppe, I. Mcculloch, U. S. Schubert, T. M. Watson, J. R. Durrant, W. C. Tsoi, J.-S. Kim, Z. Li, *Cell Rep Phys Sci* **2021**, *2*, 100498.
[21] M. Günther, D. Blätte, A. L. Oechsle, S. S. Rivas, A. A. Yousefi Amin, P. Müller-Buschbaum, T. Bein, T. Ameri, *ACS Appl. Mater. Interfaces* **2021**, *13*, 19072.
[22] W. Yang, W. Wang, Y. Wang, R. Sun, J. Guo, H. Li, M. Shi, J. Guo, Y. Wu, T. Wang, G. Lu, C. J. Brabec, Y. Li, J. Min, *Joule* **2021**, *5*, 1209.
[23] Z. Yin, S. Mei, P. Gu, H.-Q. Wang, W. Song, W. Song, *iScience* **2021**, *24*, 103027.
[24] B. Zhou, L. Wang, Y. Liu, C. Guo, D. Li, J. Cai, Y. Fu, C. Chen, D. Liu, Y. Zhou, W. Li, T. Wang, *Adv. Funct. Mater.* **2022**, *32*, 2206042.
[25] B. Fan, W. Gao, X. Wu, X. Xia, Y. Wu, F. R. Lin, Q. Fan, X. Lu, W. J. Li, W. Ma, A. K.-Y. Jen, *Nat. Commun.* **2022**, *13*, 5946.
[26] A. Labiod, O. A. Ibraikulov, S. Dabos-Seignon, S. Ferry, B. Heinrich, S. Méry, S. Fall, H. J. T. Nkuissi, T. Heiser, C. Cabanetos, N. Leclerc, E. P. Lévêque, *Org. Electron.* **2022**, *107*, 106549.
[27] Q. Liao, Q. Kang, Y. Yang, Z. Zheng, J. Qin, B. Xu, J. Hou, *CCS Chem.* **2022**, *4*, 938.
[28] S. H. K. Paleti, S. Hultmark, N. Ramos, N. Gasparini, A.-H. Emwas, J. Martin, C. Müller, D. Baran, *Sol. RRL* **2022**, *6*, 2200436.
[29] L.-Y. Su, H.-H. Huang, C.-E. Tsai, C.-H. Hou, J.-J. Shyue, C.-H. Lu, C.-W. Pao, M.-H. Yu, L. Wang, C.-C. Chueh, *Small* **2022**, *18*, 2107834.
[30] P. Weitz, V. M. Le Corre, X. Du, K. Forberich, C. Deibel, C. J. Brabec, T. Heumüller, *Adv. Energy Mater.* **2022**, *13*, 2202564.
[31] Y. Wu, Q. Fan, B. Fan, F. Qi, Z. Wu, F. R. Lin, Y. Li, C.-S. Lee, H. Y. Woo, H.-L. Yip, A. K.-Y. Jen, *ACS Energy Lett.* **2022**, *7*, 2196.
[32] A. Al-Ahmad, B. Vaughan, J. Holdsworth, W. Belcher, X. Zhou, P. Dastoor, *Coatings* **2022**, *12*, 1071.
[33] P. Jiang, L. Hu, L. Sun, Z. Li, H. Han, Y. Zhou, *Chem. Sci.* **2022**, *13*, 4714.
[34] W. Greenbank, L. Hirsch, G. Wantz, S. Chambon, *Appl. Phys. Lett.* **2015**, *107*, 263301.

[35] J. Ahmad, K. Bazaka, L. J. Anderson, R. D. White, M. V. Jacob, *Renewable Sustainable Energy Rev.* **2013**, *27*, 104.
[36] T. Ahmad, S. Dasgupta, S. Almosni, A. Dudkowiak, K. Wojciechowski, *Energy Environ. Mater.* **2022**, *6*, e12434.
[37] F. Matteocci, L. Cinà, E. Lamanna, S. Cacovich, G. Divitini, P. A. Midgley, C. Ducati, A. Di Carlo, *Nano Energy* **2016**, *30*, 162.
[38] A. Uddin, M. Upama, H. Yi, L. Duan, *Coatings* **2019**, *9*, 65.
[39] K. Lochhead, E. Johlin, D. Yang, *Thin Films: Deposition Methods and Applications*, (Ed: D. Yang), IntechOpen, Rijeka **2022**.
[40] Y. He, N. Li, T. Heumüller, J. Wortmann, B. Hanisch, A. Aubele, S. Lucas, G. Feng, X. Jiang, W. Li, P. Bäuerle, C. J. Brabec, *Joule* **2022**, *6*, 1160.
[41] Z. Ma, Y. Dong, Y.-J. Su, R. Yu, H. Gao, Y. Gong, Z.-Y. Lee, C. Yang, C.-S. Hsu, Z. Tan, *ACS Appl. Mater. Interfaces* **2022**, *14*, 1187.
[42] H. Cha, J. Wu, *Joule* **2021**, *5*, 1322.
[43] S. B. Dkhil, M. Pfannmöller, M. I. Saba, M. Gaceur, H. Heidari, C. Videlot-Ackermann, O. Margeat, A. Guerrero, J. Bisquert, G. Garcia-Belmonte, A. Mattoni, S. Bals, J. Ackermann, *Adv. Energy Mater.* **2017**, *7*, 1601486.
[44] Y. Chen, J. Wan, G. Xu, X. Wu, X. Li, Y. Shen, F. Yang, X. Ou, Y. Li, Y. Li, *Sci China Chem* **2022**, *65*, 1164.
[45] X. Fan, J. Wang, H. Wang, X. Liu, H. Wang, *ACS Appl. Mater. Interfaces* **2015**, *7*, 16287.
[46] K. Burlafinger, S. Strohm, C. Joisten, M. Woiton, A. Classen, J. Hepp, T. Heumüller, C. J. Brabec, A. Vetter, *Prog. Photovoltaics* **2022**, *30*, 518.
[47] M. Hermenau, *Lebensdaueruntersuchungen an Organischen Solarzellen*, German National Library, Dresden, Germany **2012**.
[48] Y. Li, T. Li, Y. Lin, *Mater. Chem. Front.* **2021**, *5*, 2907.
[49] L. J. Sutherland, H. C. Weerasinghe, G. P. Simon, *Adv. Energy Mater.* **2021**, *11*, 2101383.
[50] X. Xu, D. Li, J. Yuan, Y. Zhou, Y. Zou, *EnergyChem* **2021**, *3*, 100046.
[51] D. Luo, W. Jang, D. D. Babu, M. S. Kim, D. H. Wang, A. K. K. Kyaw, *J. Mater. Chem. A* **2022**, *10*, 3255.
[52] L. Duan, A. Uddin, *Adv. Sci.* **2020**, *7*, 1903259.
[53] X. Hou, Y. Wang, H. K. H. Lee, R. Datt, N. Uslar Miano, D. Yan, M. Li, F. Zhu, B. Hou, W. C. Tsoi, Z. Li, *J. Mater. Chem. A* **2020**, *8*, 21503.
[54] S. Alem, R. Aich, J. Lu, N. Graddage, F. Zhang, Y. Tao, *Sol. Energy* **2021**, *230*, 791.
[55] D. E. Carlson, K. Rajan, *Appl. Phys. Lett.* **1997**, *70*, 2168.
[56] M. V. Khenkin, A. K. M., E. A. Katz, I. Visoly-Fisher, *Energy Environ. Sci.* **2019**, *12*, 550.
[57] M. V. Khenkin, E. A. Katz, A. Abate, G. Bardizza, J. J. Berry, C. Brabec, F. Brunetti, V. Bulović, Q. Burlingame, A. Di Carlo, R. Cheacharoen, Y.-B. Cheng, A. Colsmann, S. Cros, K. Domanski, M. Dusza, C. J. Fell, S. R. Forrest, Y. Galagan, D. Di Girolamo, M. Grätzel, A. Hagfeldt, E. von Hauff, H. Hoppe, J. Kettle, H. Köbler, M. S. Leite, S. Liu, Y.-L. Loo, J. M. Luther, et al., *Nat. Energy* **2020**, *5*, 35.
[58] C.-Y. Liao, Y. Chen, C.-C. Lee, G. Wang, N.-W. Teng, C.-H. Lee, W.-L. Li, Y.-K. Chen, C.-H. Li, H.-L. Ho, P. H.-S. Tan, B. Wang, Y.-C. Huang, R. M. Young, M. R. Wasielewski, T. J. Marks, Y.-M. Chang, A. Facchetti, *Joule* **2020**, *4*, 189.
[59] M. Glatthaar, M. Niggemann, B. Zimmermann, P. Lewer, M. Riede, A. Hinsch, J. Luther, *Thin Solid Films* **2005**, *491*, 298.
[60] D. Kaduwal, H.-F. Schleiermacher, J. Schulz-Gericke, T. Kroyer, B. Zimmermann, U. Würfel, *Sol. Energy Mater. Sol. Cells* **2014**, *124*, 92.
[61] C.-Y. Liao, Y.-T. Hsiao, K.-W. Tsai, N.-W. Teng, W.-L. Li, J.-L. Wu, J.-C. Kao, C.-C. Lee, C.-M. Yang, H.-S. Tan, K.-H. Chung, Y.-M. Chang, *Sol. RRL* **2021**, *5*, 2000749.
[62] Y.-M. Sung, Y.-C. Huang, F. S.-S. Chien, C.-S. Tsao, *IEEE J. Photovoltaics* **2019**, *9*, 694.
[63] H. J. Son, H.-K. Park, J. Y. Moon, B.-K. Ju, S. H. Kim, *Sustainable Energy Fuels* **2020**, *4*, 1974.
[64] M. Tessarolo, A. Guerrero, D. Gedefaw, M. Bolognesi, M. Prosa, X. Xu, M. Mansour, E. Wang, M. Seri, M. R. Andersson, M. Muccini, G. Garcia-Belmonte, *Sol. Energy Mater. Sol. Cells* **2015**, *141*, 240.
[65] L. Duan, H. Yi, Y. Zhang, F. Haque, C. Xu, A. Uddin, *Sustainable Energy Fuels* **2019**, *3*, 723.
[66] H. Lee, J. Sohn, P. Tyagi, C. Lee, *Appl. Phys. Lett.* **2017**, *110*, 53301.
[67] M. Ghasemi, N. Balar, Z. Peng, H. Hu, Y. Qin, T. Kim, J. J. Rech, M. Bidwell, W. Mask, I. McCulloch, W. You, A. Amassian, C. Risko, B. T. O'Connor, H. Ade, *Nat. Mater.* **2021**, *20*, 525.